Wiley
Applied and Environmental Soil Science
Volume 2025, Article ID 8848852, 19 pages
https://doi.org/10.1155/aess/8848852

WILEY

Research Article

Modeling the Hydrological Process of the Genale Dawa-3 Dam Watershed, Ethiopia

Ashenafi Dechasa,[1] **Wakjira T. Dibaba**,[2] **Alemu O. Aga**,[3] **Mezgebu Geme Worku**,[1] **Miliyon Dida Feye**,[1] **Firaol Bedada Kopesa**,[4] **Bekele Terefe Gebisa**,[1] **Brook Legese**,[5] **and Amare Tura Abate**[1]

[1]*Department of Hydraulic and Water Resources Engineering, Bule Hora University, Bule Hora, Ethiopia*
[2]*Department of Hydraulic and Water Resources Engineering, Jimma University, Jimma, Ethiopia*
[3]*Department of Water Works Construction Technology, Ethiopia Technical University (FTVTI), Addis Ababa, Ethiopia*
[4]*Department of Civil Engineering, Ambo University, Woliso Campus, Woliso, Ethiopia*
[5]*Department of Natural Resource Management, Bule Hora University, Bule Hora, Ethiopia*

Correspondence should be addressed to Ashenafi Dechasa; ashenafi.dechasa@bhu.edu.et

Received 25 April 2024; Revised 2 December 2024; Accepted 18 December 2024

Academic Editor: Venkatramanan Senapathi

Watershed hydrology comprehension is fundamental to the efficacious management of water resources and the formulation of sustainable solutions. This research used the soil and water assessment tool (SWAT) to analyze the hydrological dynamics of the Genale Dawa-3 dam watershed, to advance sustainable water management strategies. Model calibration and validation were performed using sequential uncertainty fitting (SUFI-2) within SWAT-CUP, and performance was assessed through various statistical measures including R^2, NSE, PBIAS, and RSR. The findings demonstrated a robust correlation between observed and simulated streamflow during both the calibration and validation stages. The statistical analysis revealed that there was significant agreement between the observed and simulated streamflow in terms of R^2 (0.79, 0.75), NSE (0.74, 0.72), PBIAS (−2.8, 2.1), and RSR (0.57, 0.56) during calibration and validation. Evapotranspiration was found to account for 64.66% of precipitation loss, while surface runoff, groundwater flow, and water yield were each responsible for 12.62%, 9.47%, and 32.28% of the annual water balance, respectively. A yearly water balance analysis revealed that evapotranspiration was the primary route of precipitation loss, followed by surface runoff, groundwater movement, and overall water yield. The study estimated the total water potential of the watershed to be 2.45 BMC. Notable spatial heterogeneity in water balance components was observed across subwatersheds, attributable to variations in pedological characteristics, land use/land cover patterns, topographical features, and precipitation distribution. The elucidated hydrological processes provide a robust empirical framework for water resource practitioners and policymakers to formulate and implement evidence-based, sustainable management strategies.

Keywords: Genale Dawa-3; hydrological process; SWAT; watershed

1. Introduction

Effective water resource management is crucial for meeting current demands and ensuring sustainability, as freshwater resources are limited, irregular, and unevenly distributed in relation to population [1]. Ethiopia, designated as the "water tower of North–east Africa," is characterized by complex topographical features, with surface water predominantly originating from precipitation-induced runoff processes along mountainous gradients [2]. Hydrological processes in watersheds are significantly impacted by variations in precipitation and temperature, leading to more severe flooding, extended droughts, and increased water scarcity. To comprehend the underlying mechanisms governing water flow

and its effects on water quantity and quality, hydrological studies in river basins are crucial [3]. However, assessing hydrological processes presents significant challenges in developing countries with limited hydroclimatic data availability, such as the Genale Dawa basin. In this context, water balance analyses provide crucial insights into watershed hydrological characteristics and facilitate the identification of temporal variations in key hydrological processes [4]. The quantification of water generation processes in river basins is fundamental to effective resource management, particularly given that conventional methodologies for hydrological parameter estimation often exhibit limitations in reliability and temporal efficiency [5]. Therefore, appropriate methodologies and databases are essential for accurately measuring hydrological process characteristics, enabling effective water resource management. Sustainable water resource management requires regulating water usage by understanding basin water supply and balancing increasing demands with environmental protection. This necessitates a comprehensive management approach encompassing policy development, administrative and functional organization, and management systems in government and private institutions.

The temporal and spatial heterogeneity of river flows, coupled with increasing demand, underscores the criticality of accurate water availability estimation for the effective implementation of water resource management tools. The significance of water management is intrinsically linked to environmental sustainability parameters, influenced by diverse policy frameworks and socioeconomic factors within the watershed context [6]. The emergence of freshwater as a universal systemic concern is evidenced by resource scarcity and unsustainable exploitation patterns [7]. Addressing these issues necessitates integrated water resource management, with the modeling of watershed hydrological processes being a critical aspect of achieving sustainable water resource usage.

Hydrological models have been developed to oversee water resource management by studying the spatiotemporal variation of water resources, with the primary goal of providing insights for sustainable management through hydrological assessment [8]. Water resource management has become increasingly vital and complex as a result of competing stakeholder demands, rapid population growth, industrialization, hydropower development, irrigation, urbanization, and land degradation [9]. In such circumstances, water balance studies offer insights into the hydrological features of watersheds and are used to detect changes in crucial hydrological processes. The key elements of a basin's water balance include precipitation, surface runoff (SUR_Q), lateral flow (LAT_Q), base flow, and evapotranspiration. Except for precipitation, all these variables are difficult to measure and require prediction to be quantified [10]. Hydrologists and water managers must incorporate the latest land use and land cover (LULC) data into hydrologic calculations and runoff modeling for accurate assessments [11]. In addition, a watershed's hydrological processes are impacted by geography, geology, weather, land use, and human activity.

Numerous hydrological studies have been conducted in the Upper Blue Nile basin, including investigations in the Upper Blue Nile basin [4, 5], Nashe Watershed [8], Upper Guder catchment [12], Guder catchment [13], Finchaa catchment [14], and Koga watershed [15] to simulate and evaluate the water resource potential of the basin. According to the studies, the soil and water assessment tool (SWAT) model has been effective in addressing a broad spectrum of hydrological processes and water quality challenges across different watershed sizes and environmental contexts, particularly for scenarios requiring detailed hydrological simulations and enhancements. Numerous researchers have used the SWAT model to analyze the hydrological process of various Ethiopian basins and around the world. For instance [12], employed the SWAT model to simulate streamflow in the upper Guder catchment. Similarly [15], applied the SWAT model to predict streamflow and sediment yield in the Koga watershed, achieving effective calibration and validation. Additionally [8], used the SWAT model to simulate the hydrological characteristics of the Nashe watershed, yielding satisfactory results. Despite extensive research, the hydrological processes in the Genale Dawa-3 dam watershed remain inadequately investigated, with evidence indicating severe soil erosion, sedimentation patterns, and increased watershed vulnerability to drought conditions. To address this knowledge gap, this study was conducted using a physical-based semidistributed SWAT to simulate and evaluate hydrological processes in the Genale Dawa-3 dam watershed. The study also identified the spatial distribution of water balance components in the watershed.

The research outcomes are expected to enhance water resource management in the entire basin and alleviate water-related problems. Consequently, understanding the hydrological processes in the Genale Dawa-3 dam watershed is critical for managing sustainable water resource projects in the area. In conclusion, this study stands out for its unique approaches, comprehensive data integration frameworks, and substantial contributions to hydrological understanding and management of water resources in the Genale Dawa-3 dam watershed. These advancements not only improve scientific knowledge but also compromise practical tools for sustainable water management in Ethiopia and other regions experiencing water scarcity. Beyond its scientific contributions to hydrological modeling, this research provides actionable insights for water resource management. Its detailed analysis of hydrological processes and interactions establishes a foundation for future research on improving water security and sustainability in similarly challenged regions worldwide.

2. Materials and Methods

2.1. Description of the Research Area

2.1.1. Location and Topography. The Genale-Dawa River Basin, situated in southeastern Ethiopia, is one of the country's major drainage basins, encompassing an area of approximately 1,72,880 km^2 [16]. It ranks as Ethiopia's

third-largest basin after the Abbay and Wabeshebele Rivers, comprising 15.3% of the nation's total area [17]. The focus of this research, the Genale Dawa-3 dam watershed, is located in the middle section of the Genale River, roughly 655 km from Addis Ababa, within the broader Genale Dawa River basin. This study area covers a drainage area of 10,264 km^2 and is positioned at 5°38′ N latitude and 39°43′ E longitude. A visual representation of the study area is provided in Figure 1 [18], with the digital elevation map sourced from [19].

The Genale Dawa-3 dam watershed exhibits significant topographical variation, with elevations ranging from 1039 to 3751 m above sea level. This diverse landscape is characterized by a predominance of highlands and plateaus, interspersed with volcanic formations and steep inclines. The terrain transitions to gentle lowlands that extend to the bases of escarpments, and floodplains are found in the lower elevation areas [18]. This topographical diversity contributes to the watershed's complex hydrological processes and influences its water resource distribution.

2.1.2. Climate. The Genale Dawa-3 dam watershed exhibits a complex bimodal rainfall pattern with two distinct rainy seasons. The Type I bimodal pattern spans approximately 7 months from April to October, with less pronounced precipitation peaks at the beginning and end. In contrast, the Type II bimodal pattern shows less distinct rainfall peaks in April and October, with minimal precipitation between these peaks at Kibremengist, Negele, and Dellomena stations. The highest rainfall between these peaks occurs at Hagerselam, Bore, Worka, and Yirbamuda stations (Figure 2). Average annual rainfall within the watershed varies significantly, ranging from 1334.61 mm to 633.47 mm (Figure 3). The temperature in the region remains relatively stable, with only minor monthly fluctuations. Mean monthly maximum temperatures range between 18°C and 26°C (Figure 4), while minimum temperatures vary from 6°C to 15°C (Figure 5). Annually, the average maximum temperature is approximately 22°C, with an average minimum of about 10.5°C. The watershed's climate patterns are further differentiated by geography, with the northern and highland areas experiencing three distinct wet seasons (March to May, June to September, and September to November), while the southeastern and lowland sections have two wet seasons. This diverse climatic profile significantly influences the hydrological processes within the Genale Dawa-3 dam watershed. The initial season extends from March through May, with April typically being the wettest month, and the latter season occurs from September to November, with October often seeing the highest rainfall. The primary river, Genale, has its sources in the Sidamo Mountains to the northwest and the Bale Mountains massif to the northeast [16, 18, 20].

2.2. SWAT Model Inputs. A SWAT model was employed to analyze the hydrological characteristics of the Genale Dawa-3 dam watershed. This model incorporated various spatial and temporal datasets, such as the Digital Elevation Model (DEM), soil information, LULC data, and meteorological records. Following its development and configuration, the model underwent calibration and validation processes using streamflow measurements.

2.2.1. DEM of the Study Area. A DEM with 30×30 m resolution was the main input for the SWAT model, helping to understand flow patterns and behavior. The DEM provided detailed elevation data for specific points across the area, allowing for watershed boundary delineation and land surface drainage analysis. From this DEM, various terrain parameters were derived, including slope gradient and length, as well as stream network characteristics like channel slope, length, and width. The SWAT model utilized this DEM to evaluate flow accumulation and define stream networks within the watershed. This process segmented the watershed into various sub-basins based on elevation, as illustrated in Figure 1 and downloaded from the NASA website [19].

2.2.2. LULC Map. The influence of LULC patterns on watershed dynamics, including soil loss, water flow, sediment transport, and moisture evaporation, is well-established in hydrological modeling [21]. For this research, LULC information was extracted from Landsat 8 Operational Land Imager (OLI) data. Researchers accessed a cloud-free satellite image of the study area through the US Geological Survey (USGS) online portal [22]. The image underwent classification using ERDAS IMAGINE 2015 software, with subsequent mapping carried out in ArcGIS 10.3. A supervised classification approach was employed to generate the LULC map, and its precision was evaluated using a confusion matrix. This assessment yielded an overall accuracy of 91.2% and a kappa coefficient of 0.8703. The Genale Dawa-3 dam watershed exhibited six primary LULC categories: croplands, shrublands and grasslands, forested areas, urban zones, aquatic features, and exposed terrain. The LULC distribution analysis revealed that agricultural land dominated the landscape, covering 61.11% of the total area. This was followed by shrublands and grasslands at 20.68%, forested regions at 14.74%, urban development at 1.68%, water bodies at 1.3%, and barren areas at 0.48%. The prevalence of agricultural land, with shrublands and grasslands as the second most common category, was visually represented in Figure 6.

2.2.3. Soil Map. Soil data is essential for the Arc SWAT model, providing various parameters that indicate soil hydrological and textural properties, as well as soil type distribution in the watershed. The SWAT model requires specific physicochemical and textural soil characteristics, including available water content, bulk density, hydraulic conductivity, soil texture, and organic carbon content for each soil type [23]. For this study, soil data was sourced from the soil map of Ethiopia, Oromia Water Works Design, and Supervision Enterprise (OWWDSE) [24]. The major soil types identified were chromic cambisols, chromic luvisols,

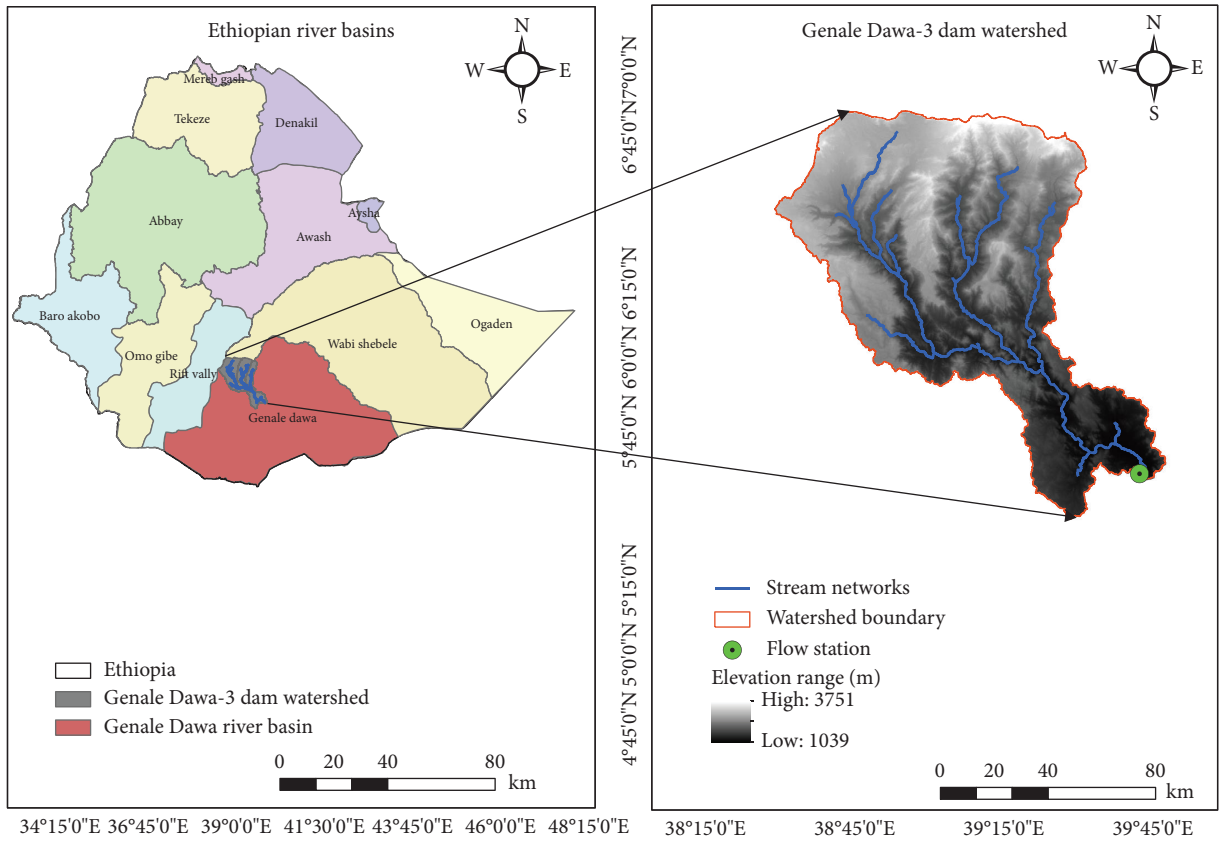

Figure 1: Map of the study area.

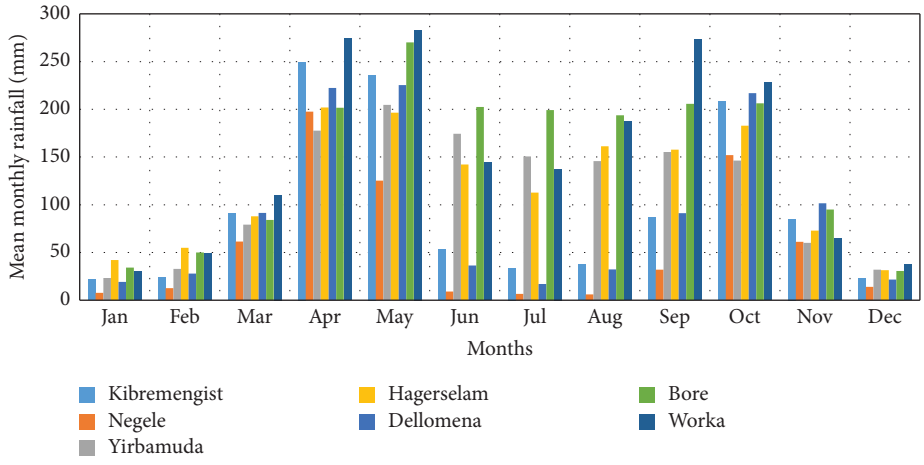

Figure 2: Mean monthly rainfall of selected stations in the study area (1987–2019).

eutric cambisols, eutric leptosols, eutric vertisols, haplic luvisols, humic nitisols, and lithic leptosols. Chromic luvisols, characterized by loam textural properties, were found to be the dominant soil type, covering 50.13% of the watershed area (Figure 7).

2.2.4. Weather Data. The SWAT hydrological model relies on daily meteorological inputs to simulate water balance dynamics. These inputs encompass precipitation, temperature extremes, atmospheric moisture content, wind velocity, and solar energy flux. For this study, the requisite climate data was sourced from the Ethiopian National Meteorological Agency (NMA) [25]. While temperature and rainfall measurements were accessible across all monitoring sites, comprehensive weather parameters were only available from the Kibremengist station. At this location, which provided daily records of sunshine duration, researchers employed an empirical conversion method to derive the solar radiation values necessary for SWAT model implementation. This conversion

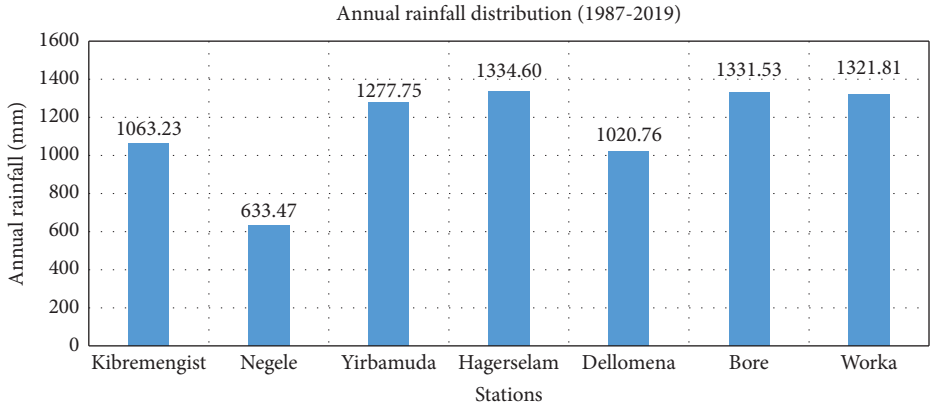

Figure 3: Mean annual rainfall distribution of selected stations in the study area (1987–2019).

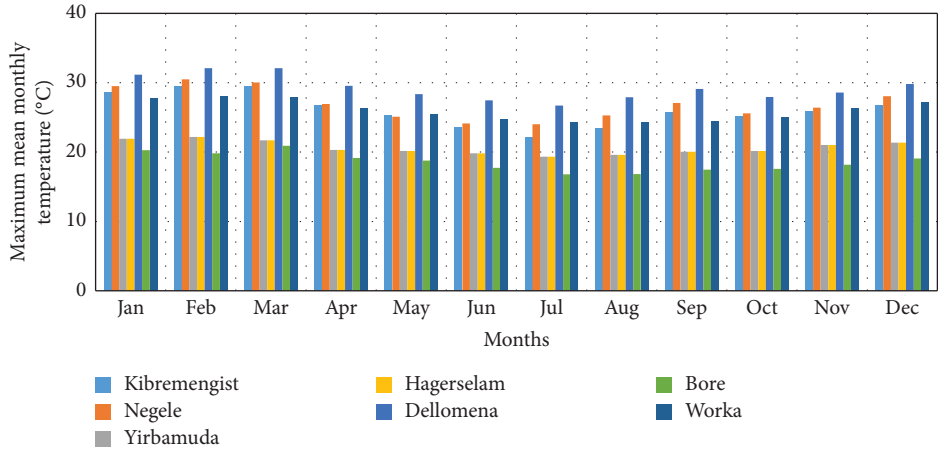

Figure 4: The maximum mean monthly temperature of selected stations in the study area (1987–2019).

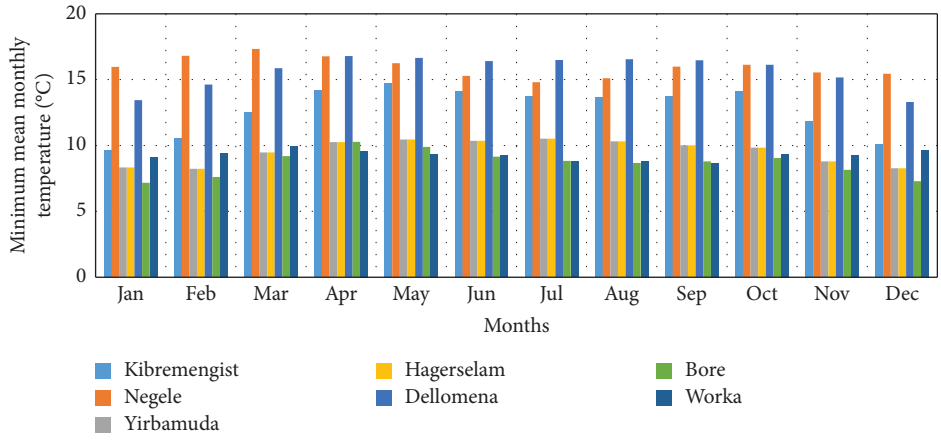

Figure 5: The minimum mean monthly temperature of selected stations in the study area (1987–2019).

technique, detailed in [26], transformed sunshine hours into the required daily solar radiation estimates. The study utilized data from seven meteorological stations (Table 1). Missing data was filled using multiple imputation techniques (MCMC) in XLSTAT2019. To ensure data quality, homogeneity, and consistency tests were conducted using the Pettis algorithm and double mass curve (DMC) technique, respectively. All chosen meteorological stations were found to be homogeneous (uniform) and consistent (reliable). The Kibremengist station served as the primary (synoptic) station for generating meteorological data for other stations in the research area.

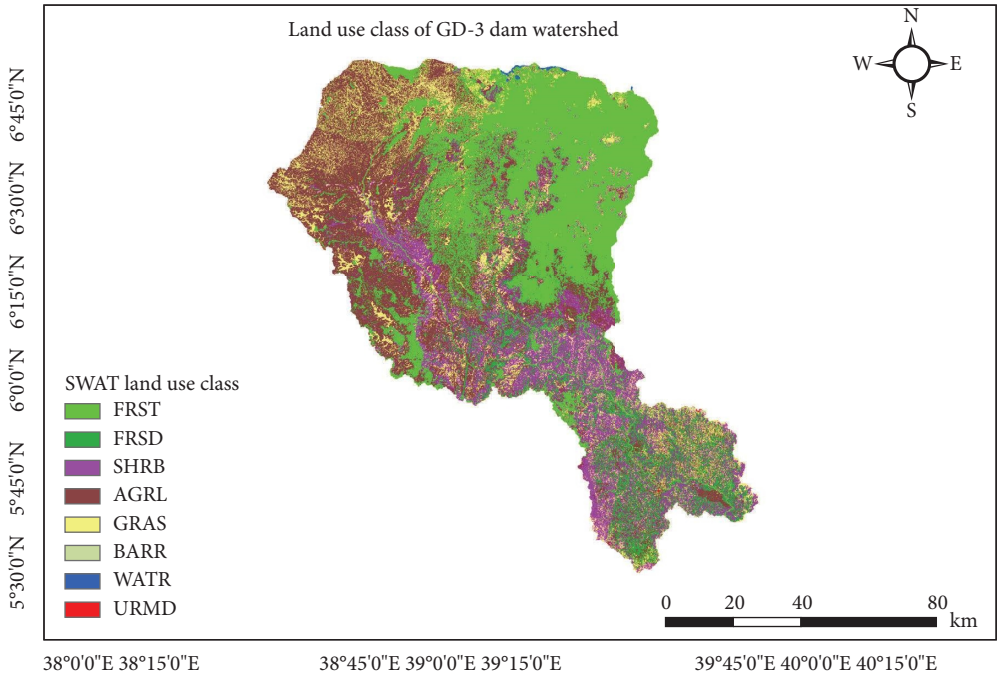

Figure 6: Map of land use in the watershed of the Genale Dawa-3 dam.

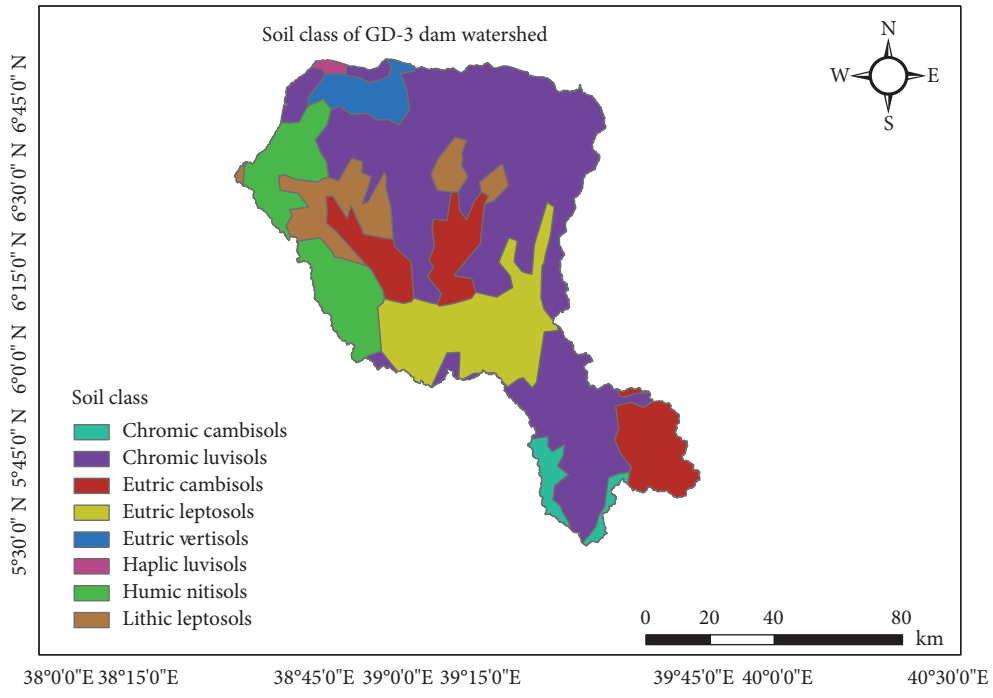

Figure 7: Soil map of the Genale Dawa-3 dam watershed.

2.2.5. River Flow Data. The streamflow measurements made at the Chenemasa hydrological gauge station between 1990 and 2015 and transposed to the Genale Dawa-3 dam outlet, were collected from the Ministry of Water and Energy of Ethiopia (MoWE) [27]. Before starting a hydrological study, it is crucial to verify that the data are sufficient, adequate, homogeneous, and free of missing information. In addition, before checking the homogeneity test, outlier test, and data preparation for the calibration and validation process, some missing data were filled. Several methods are available for estimating missed streamflow data. For this research, XLSTAT2019 (Excel add-ins) was used to fill in missing streamflow data by MCMC. To ensure data quality control test, both homogeneity and outlier tests were conducted using the Pettis algorithm and logarithmic technique, respectively. For this study, 26 years of measured river flow

Table 1: Meteorological stations in the watershed of the Genale Dawa-3 dam (1987–2019).

No	Stations	Lat. (°N)	Long. (°E)	Elev (m)	Weather elements					
					RF	T_{max}	T_{min}	RH	SS	WS
1	Kibremengist	5.87	38.97	1680	√	√	√	√	√	√
2	Negele	5.42	39.57	1544	√	√	√	√	NA	NA
3	Bore	6.35	38.62	2712	√	√	√	NA	NA	NA
4	Worka	6.48	39.21	2450	√	√	√	NA	NA	NA
5	Yirbamuda	6.2	38.71	2569	√	√	√	NA	NA	NA
6	Hagerselam	6.49	38.52	2809	√	√	√	NA	NA	NA
7	Dellomena	6.42	39.83	1313	√	√	√	NA	NA	√

Note: the abbreviations used are as follows: √ indicates Data Availability, and NA indicates Data Unavailability.
Abbreviations: Elev, elevation; Lat., latitude; Long., longitude, RF, rainfall; RH, relative humidity; SS, sunshine; T_{max}, maximum temperature, T_{min}, minimum Temperature; WS, wind speed.

data were homogeneous and analyzed using an outlier test equation. The analysis confirmed that the data did not contain any extremely high or low outliers.

2.3. SWAT Model Setup. The Genale Dawa-3 dam watershed analysis incorporated high-resolution topographic mapping at 30 m grid cell resolution. Through the application of a threshold area of 17,250 ha, the 10,264 km^2 watershed domain was systematically delineated into 31 distinct sub-basins (Figure 8). Further analysis led to the identification of 253 hydrologic response units (HRUs), each representing a unique combination of land use, soil type, and topography. These HRUs were established using threshold criteria of 10% for both land use and soil classifications, and 15% for slope categories. The topographic assessment revealed a predominantly steep terrain profile, with slopes exceeding 15% gradient characterizing more than 60% of the watershed terrain. This complex topographical configuration plays a fundamental role in governing regional hydrological processes and watershed dynamics.

2.4. SWAT Model Description. SWAT, as described by [28], is a semidistributed physically based model used to evaluate the effects of land management practices on water resources, sediment transport, and agricultural chemical yields. The model addresses watersheds with heterogeneous soil compositions, diverse land use patterns, and varied management practices over extended temporal scales. To enhance prediction accuracy, the model incorporates geographic variability parameters, thereby minimizing errors associated with lumped and linear system assumptions [29].

Within the basin framework, each sub-basin is divided into HRUs characterized by uniform land use patterns, management protocols, topographical features, and soil properties [28]. This systematic subdivision proves essential for regions exhibiting distinct characteristics that influence hydrological processes, enabling comparative analysis between diverse basin segments with unique environmental attributes.

SWAT simulates runoff and sediment transport at the HRU level and then routes water and sediments through the stream network to the basin outlet [29]. The hydrological components for each HRU were simulated using the water balance equation (equation (1))

$$SW_t = SW_0 + \sum_{i=1}^{t} \left(R_{\text{day}} - Q_{\text{surf}} - E_a - W_{\text{seep}} - Q_{qw}\right), \quad (1)$$

where SW_t is the final content of soil water (mm), SW_0 is the amount of soil water at the start of day i (mm), t is the number of days, R_{day} is the precipitation on day i (mm), Q_{surf} is the SUR_Q on day i (mm), E_a is the evapotranspiration on day i (mm), W_{seep} is the water entering the vadose zone from the soil profile on day i (mm), and Q_{qw} is the return flow amount on day i (mm).

The Soil Conservation Services (SCS) curve number approach is used in the SWAT model to simulate runoff in the watershed [30]. The SUR_Q is estimated using equation (2):

$$Q_{\text{surf}} = \frac{\left(R_{\text{day}} - I_a\right)^2}{\left(R_{\text{day}} - I_a + S\right)}, \quad (2)$$

where Q_{surf} is the accumulated runoff or excess rainfall (mm); R_{day} is the daily rainfall depth (mm); I_a is an initial abstraction that includes surface storage, interception, and infiltration before runoff (mm); and S is the retention parameter (mm). Due to variations in soil, land use, and management, as well as temporary changes in soil water content (SWo), the retention parameter varies spatially. Empirically, retention is calculated by using equation (3):

$$S = 25.4\left(\frac{1000}{CN} - 10\right), \quad (3)$$

where CN is the curve number for the day. The initial abstraction, Ia, is usually approximated as 0.2S, and equation (3) becomes:

$$Q_{\text{surf}} = \frac{\left(R_{\text{day}} - 0.2\,S\right)^2}{\left(R_{\text{day}} + 0.8\,S\right)}. \quad (4)$$

Water yield is a critical parameter for evaluating sustainable water resource management in a study area. It represents the total water volume leaving the HRU and entering the main channel during a specified timeframe [29]. The SWAT model allows for the assessment of both water yield and water balance components, which aids in water resource planning and management within a river basin [3]. The model's equation (5) specifically provides a method for calculating the total water yield for a given watershed:

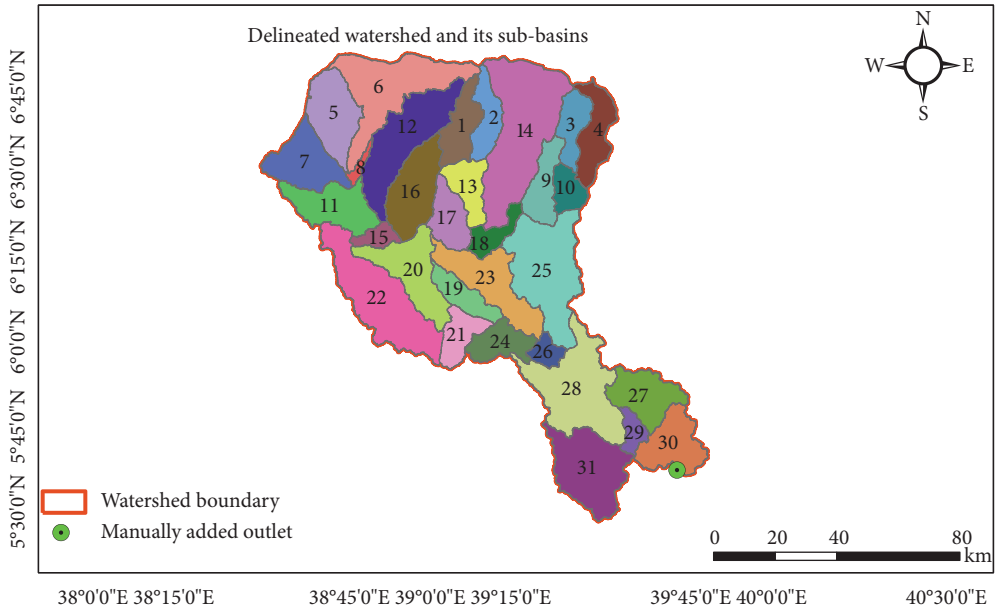

Figure 8: Delineated watershed and sub-basins of the study area.

$$W_{\text{yld}} = Q_{\text{surface}} + Q_{gw} + Q_{\text{lat}} - T_{\text{loss}} \quad (5)$$

where W_{yld} is the measure of water yield (mm), Q_{surface} is the SUR_Q(mm), Q_{lat} is the LAT_Q contribution to the stream (mm), Q_{gw} is the groundwater contribution to streamflow (mm), and T_{loss} is the transmission loss (mm) from the tributary in the HRU using transmission through the bed.

Determination of the water balance of a watershed involves consideration of several parameters, one of which is potential evapotranspiration (PET). The SWAT model used three distinct methods for calculating evapotranspiration; in this particular study, the Penman–Monteith method was selected, which incorporates the main factors such as solar radiation, air temperature, relative humidity (RH), and wind speed [31]. The Penman–Monteith equation (equation (6)) to compute the long-term PET.

$$\text{PET} = \frac{0.408\,(R_{net} - G) + \gamma\,(900/(T + 273))U\,(e_s - e_a)}{\Delta + \gamma\,(1 + 0.34U)}, \quad (6)$$

where R_{net} represents the net radiation flux measured in megajoules per square meter per day ($\text{MJm}^{-2}\cdot\text{day}^{-1}$). G denotes the heat flux density in the soil, which is minimal and can be ignored ($\text{MJm}^{-2}\cdot\text{day}^{-1}$). T indicates the average daily air temperature, expressed in degrees Celsius (°C). The psychometric constant, symbolized by γ, is calculated in kilopascals (kPa) per degree Celsius ($^{\circ}\text{C}^{-1}$). U is the wind speed, assessed at a height of 2 m, and given in meters per second (m s^{-1}). e_s Stands for the saturation vapor pressure, while e_a is derived from e_s multiplied by the RH and then divided by 100, expressed in kPa. RH is the RH, presented as a percentage (%). Finally, Δ refers to the slope of the saturation vapor pressure curve, measured in kPa per degree Celsius ($\text{KP}_a\,^{\circ}\text{C}^{-1}$).

Similarly, the model estimates groundwater flow (GW_Q) using equation (7):

$$aq_{sh,i} = aq_{sh,i-1} + W_{\text{rchrg}} - Q_{\text{revap}} - W_{\text{deep}} - W_{\text{pump},sh}, \quad (7)$$

where the water accumulated in the shallow aquifer on day I (mm) is represented by $aq_{sh,i-1}$; the water accumulated in the shallow aquifer on the day before (mm); the recharge percolating to the aquifer on day I (mm) is represented by W_{rchrg}; the water entering the soil zone on day I (mm) is by Q_{revap}; the water percolating from the shallow to the deep aquifer on day I (mm) is represented by W_{deep}; and the water is taken out of the shallow aquifer on day I (mm) is represented by $W_{\text{pump},sh}$.

2.5. SWAT Model Simulation. The SWAT simulation used weather data from 1987 to 2019. A three-year warm-up period was implemented to gather data, which is essential for eliminating initial condition effects in the model. This phase establishes the fundamental flow conditions required for accurate simulations and allows hydrological processes to reach equilibrium. Subsequently, the simulation run output data was incorporated into the database, with results stored in SWAT output files. According to [32], simulation outcomes should not be directly applied to further analysis. Instead, it is crucial to first evaluate the model's ability to accurately predict stream flow and sediment yield through sensitivity analysis, model calibration, and validation.

2.5.1. Sensitivity Analysis, Model Calibration, Validation, and Uncertainty Analysis. According to [33], sensitivity analysis can help determine which variables have the greatest impact on output variation due to input variability. By

identifying these important variables, the number of parameters that require calibration may be reduced, resulting in a reduction in the computing time needed for model calibration. Before calibrating the model in this study, a sensitivity analysis was conducted to identify the key parameters. The sensitive parameters for simulating streamflow were identified by examining parameters previously used in the Genale Dawa River Basins and other basins, as well as by referring to the SWAT documentation, Genale watershed [3], Neshe watershed [8], Simly dam watershed [10], SWAT documentation [29], SWAT CUP user manual [34], and Himalayan catchment [35].

The study employed the SWAT_CUP tool to conduct a sensitivity analysis using the sequential uncertainty fitting (SUFI-2) method. Global parameter sensitivity was evaluated based on t-statistics and p values. Parameters with larger absolute t-statistics were identified as more sensitive, while p values indicated the significance of sensitivity differences among parameters. Those parameters with p values approaching zero were considered extremely sensitive. The aim of calibrating a model is to enhance its parameter settings for specific local conditions, thereby reducing uncertainty in predictions. This calibration process focuses on identifying the best values for parameters that have been determined to be sensitive. SUFI-2 was selected due to its versatility in working with both simple and complex hydrological models, its requirement for fewer simulations, and its consideration of all potential sources of uncertainty. Model validation, on the other hand, involves evaluating a model's output against an independent dataset without making any additional adjustments that could influence the model's calibration.

The model simulation used weather data from 1987 to 2015, incorporating a three-year warm-up period to eliminate initial condition effects. The observed data was divided, with two-thirds used for calibration and one-third for validation [34]. Specifically, streamflow data from 1990–2006 (17 years) was used for calibration, while data from 2007–2015 (9 years) was used for validation.

2.5.2. Model Performance Evaluation. The SWAT model's accuracy and reliability in streamflow prediction were assessed by comparing its outputs to observed data using several statistical metrics. These included the Nash–Sutcliffe efficiency (NSE), percent bias (PBIAS), root mean square error-to-observation standard deviation ratio (RSR), and coefficient of determination (R^2). The study employed the criteria proposed by [36] to determine if the model's performance was satisfactory (Table 2). Monthly streamflow data were utilized for both calibration and validation. R^2, ranging from 0 to 1, quantifies the correlation between observed and simulated values, with one indicating a perfect match [37]. NSE evaluates the agreement between observed and simulated values relative to a 1:1 line, where 1 signifies a perfect match. Values between 0 and 1 indicate discrepancies, while negative values suggest significant prediction errors [38]. PBIAS measures the average deviation of simulated data from observed data, with smaller values indicating higher precision. Positive values suggest underestimation, while negative values imply overestimation [39]. RSR, calculated by dividing RMSE by the standard deviation of observed data, ranges from 0 to 1. Lower values closer to 0 indicate better model fit, while values near 1 suggest poor performance.

Table 2: Assessment of model performance and acceptable ranges during the calibration and validation phases for streamflow simulations [36].

Rating	R^2	NSE	RSR	PBIAS (%)
Very good	0.75–1	0.75–1	0–0.5	$< \pm 10$
Good	0.65–0.75	0.65–0.75	0.5–0.6	$\pm 10 - \pm 15$
Satisfactory	0.5–0.65	0.5–0.6	0.6–0.7	$\pm 15 - \pm 25$
Unsatisfactory	< 0.5	≤ 0.5	> 0.7	$\geq \pm 25$

$$R^2 = \frac{\left[\sum_{i=1}^{n}\left(Q_{si} - Q_{sm}\right)\left(Q_{oi} - Q_{om}\right)\right]^2}{\sqrt{\sum_{i=1}^{n}\left(Q_{si} - Q_{sm}\right)^2}\sqrt{\sum_{i=1}^{n}\left(Q_{oi} - Q_{om}\right)^2}}, \tag{8}$$

$$\mathrm{NSE} = 1 - \frac{\sum_{i=1}^{n}\left(Q_{oi} - Q_{si}\right)^2}{\sum_{i=1}^{n}\left(Q_{oi} - Q_{om}\right)^2}, \tag{9}$$

$$\mathrm{PBIAS} = \frac{\sum_{i=1}^{n}\left(Q_{oi} - Q_{si}\right)}{\sum_{i=1}^{n} Q_{oi}} * 100\%, \tag{10}$$

$$\mathrm{RSR} = \frac{\mathrm{RMSE}}{\mathrm{STDEV}_{\mathrm{ob}}} = \frac{\sqrt{\sum_{i=1}^{n}\left(Q_{oi} - Q_{si}\right)^2}}{\sqrt{\sum_{i=1}^{n}\left(Q_{oi} - Q_{sm}\right)^2}}, \tag{11}$$

where Q_{si} = simulated value, Q_{oi} = observed value, Q_{om} = average observed value, and Q_{sm} = average simulated value.

2.6. Summary of Methodology. To ensure the quality and relevance of research outcomes, it is essential to conduct a comprehensive data search and establish a well-defined, efficient methodology before commencing any research work. This preparatory phase is critical not only for effective time management but also for the overall quality and utility of the study. Figure 9 provides a summary of the methodological approach employed in this research.

3. Results and Discussion

3.1. Evaluation of the Performance of the SWAT Model

3.1.1. Sensitivity Analysis. A comprehensive global sensitivity analysis methodology was implemented to identify and quantify the relative influence of model parameters on streamflow simulation. From an initial parameter ensemble of 20 variables, statistical significance analysis based on t-statistics and p values revealed 10 parameters exhibiting substantial influence on streamflow simulations (Table 3). The sensitivity hierarchy analysis identified seven parameters demonstrating high sensitivity coefficients: baseflow alpha factor (ALPHA_BF), initial SCS curve number (CN2),

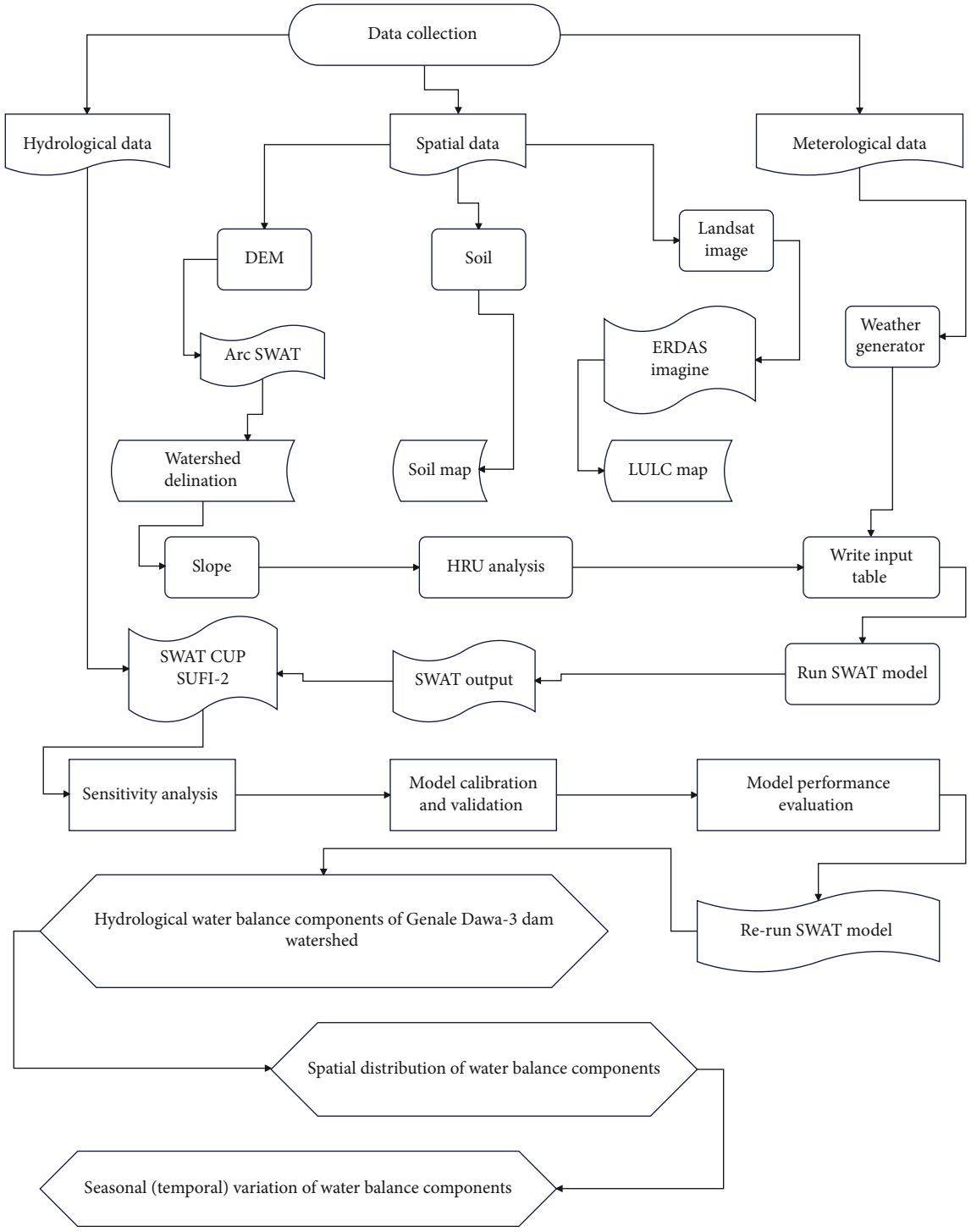

Figure 9: General conceptual framework of the study.

effective hydraulic conductivity in main channel alluvium (CH_K2), groundwater delay time (GW_DELAY), deep aquifer percolation fraction (RCHRG_DP), average slope length (SLSUBBSN), and available water capacity of the soil layer (SOL_AWC). Additionally, three parameters exhibited moderate sensitivity: average slope steepness (HRU_SLP), groundwater revap coefficient (GW_REVAP), and threshold depth of water in the shallow aquifer required for return flow (GWQMN). The identified hierarchical sensitivity patterns demonstrate notable concordance with previous investigations conducted across various Ethiopian basins, including analogous findings from the Genale watershed [3], Nashe watershed [8], Gidabo watershed [31], Lake Tana Basin [40], Gumara watershed [41], Finchaa catchment [42], Awata watershed [43], Upper Genale River basin [23], and Koga watershed [15].

Table 3: List of parameters used for streamflow calibration with their parameter ranges, fitted values, and sensitivity ranks.

Parameter name	Description of parameter	Range	Fitted value	Rank
v_ALPHA_BF.gw	Baseflow alpha factor (days)	0–1	0.94	1
r_CN2.mgt	Initial SCS CN(II) value	±25%	0.08	2
a_CH_K2.rte	Channel effective hydraulic conductivity (mm h^{-1})	0–150	96.45	3
a_GW_DELAY.gw	Groundwater delay (days)	±10	−5.95	4
v_RCHRG_DP.gw	Deep aquifer percolation fraction	0–1	0.11	5
v_SLSUBBSN.hru	Average slope length	10–150	57.69	6
r_SOL_AWC(.).sol	Available water capacity of the soil layer (mm mm^{-1})	±25%	0.23	7
r_HRU_SLP.hru	Average slope steepness	0–1	0.38	8
a_GW_REVAP.gw	Groundwater "revap" coefficient	±0.036	−0.009	9
v_GWQMN.gw	Threshold depth of water in the shallow in the shallow aquifer needed for return flow to occur (mm)	0–5000	2044.65	10

Note: The v_Replace method involves replacing an existing parameter value with a user-specified value. On the other hand, the r_Relative method multiplies the existing parameter value by (1± the given value), while the a_Absolute method involves adding the given value to the fundamental value.

3.1.2. Model Calibration and Validation. The SWAT model was automatically calibrated and validated at the watershed outlet using the most sensitive parameters. A strong correlation between observed and simulated discharges was confirmed through graphical techniques and quantitative metrics. The model's performance for streamflow calibration and validation at the Genale Dawa-3 dam watershed outlet was deemed good according to established criteria, with R^2 of 0.79 (0.75), NSE of 0.74 (0.72), PBIAS of −2.8% (+2.1%), and RSR of 0.57 (0.56) for calibration and validation, respectively (Table 2). PBIAS analysis indicated slight overestimation during calibration and underestimation during validation. These statistical performance indicators aligned with similar studies in various Ethiopian basins [23, 36, 43]. SUFI-2 uncertainty analysis yielded a *p*-factor of 0.67 and an r-factor of 0.78 for calibration, and a *p*-factor of 0.65 and an *r*-factor of 0.72 for validation at the watershed outlet (Table 4). These results indicate that the 95PPU captured 67% of observed data during calibration and 65% during validation, with high confidence (*r*-factor < 1) in both instances.

The SWAT model demonstrates a generally accurate prediction of streamflow ranges, as evidenced by graphs of monthly streamflow during calibration (Figure 10) and validation periods (Figure 11), with the overall performance shown in Figure 12. However, the model consistently underestimated peak flows, particularly during validation years, while successfully capturing the rising and falling streamflow patterns in most instances. These observations align with findings from previous research in the Toba watershed [44]. The underestimation of peak streamflow by SWAT is a common issue noted in various studies [3, 36, 45]. This discrepancy may be attributed to SWAT's simplified representation of complex hydrological processes, particularly those related to flow routing and hydrological connectivity, which can impact its accuracy during extreme conditions [3]. Additionally, the second storm effect within the SWAT model has been identified as a significant source of error contributing to peak flow underestimation [42].

This issue arises when SWAT handles consecutive storm events that occur in close temporal proximity. Essentially, if the soil and landscape have not had sufficient time to return to baseline conditions after the first storm before the second storm arrives, the model may not accurately account for the altered hydrological conditions. This includes factors like increased soil saturation, which can significantly affect runoff dynamics and hence peak flow predictions. SWAT might struggle to simulate the cumulative impact of back-to-back storms, leading to substantial underestimations of peak flow. This limitation underscores the need for enhancing the model's ability to dynamically integrate successive hydrological events within short time frames for more precise predictions. The study conducted by [45] reported that the representation of hydraulic Structures and human activities in the watershed; hydraulic structures such as dams, levees, and channels play crucial roles in influencing flow rates within a watershed. If these features are not accurately represented in the SWAT model, or if the model does not incorporate real-time operational protocols for managing these structures, the accuracy of predictions for maximum flow could be compromised. This omission can lead to significant discrepancies in modeling results, especially during extreme weather events when the management of water flow through these structures becomes critical.

For more reliable predictions, it is essential to integrate detailed, site-specific information about these hydraulic structures into the model. Additionally, simulating the operational decisions (such as dam release schedules) in real-time can further enhance the model's performance in predicting how these structures will impact flood peaks and overall water management. The researchers, as referenced in studies [3, 18], concluded that discrepancies between observed and simulated hydrographs can largely be attributed to several key factors. Firstly, the lack of detailed information on water use can significantly impact the accuracy of hydrological simulations. Without precise data on how water is extracted, used, and managed within the watershed, it is challenging to accurately model water flow and availability. Secondly, the representation of topography by DEMs is crucial for accurate water flow modeling. If the DEMs used are not high enough resolution or fail to capture critical topographical features accurately, the flow paths and water accumulation areas could be misrepresented, leading to errors in the simulated hydrograph. Lastly, spatial resolution and scale issues, particularly in representing soil types and

Table 4: The index values for the statistical properties in the monthly streamflow calibration, validation processes, and model uncertainty measurements.

Variable	Uncertainty measures		Model performance indicators			
	p-factor	*r*-factor	R^2	NSE	PBIAS	RSR
Calibration period (1990–2006)	0.67	0.78	0.79	0.74	−2.8	0.57
Validation period (2007–2015)	0.65	0.72	0.75	0.72	+2.1	0.56

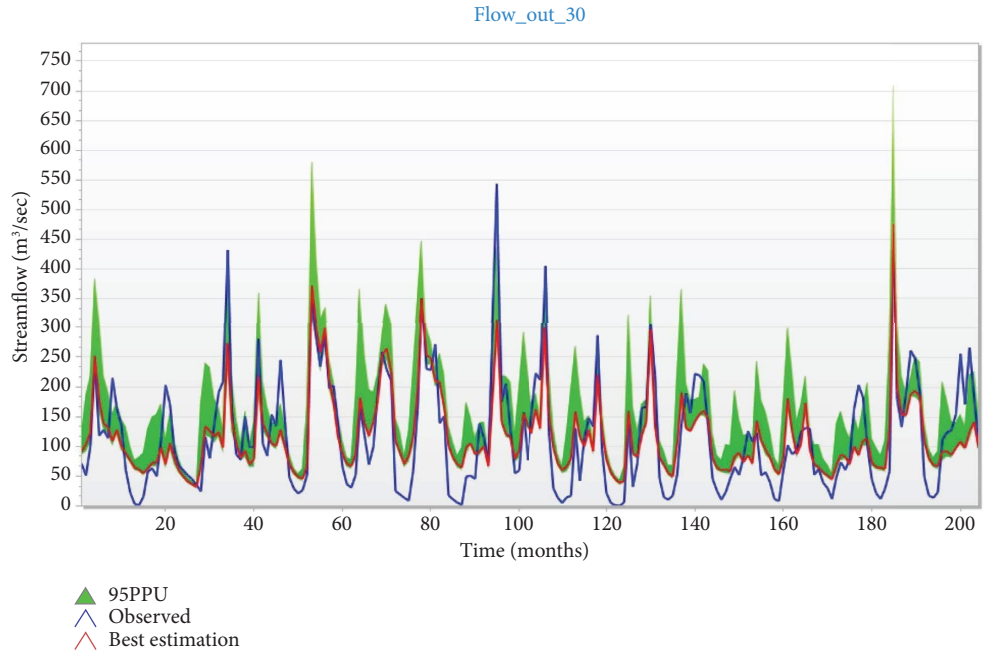

Figure 10: Monthly streamflow calibration (1990–2006).

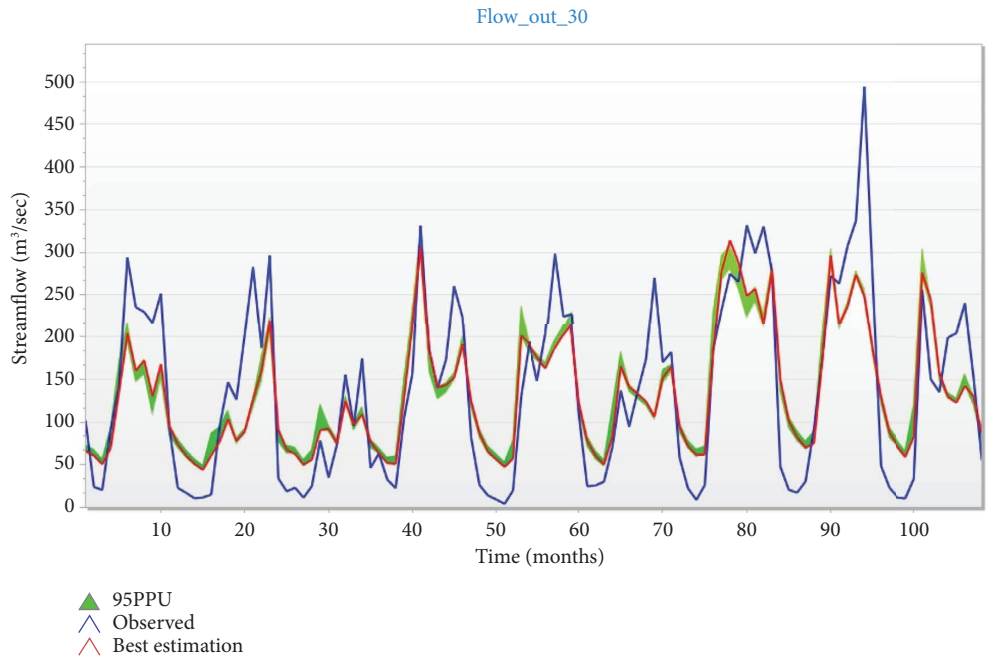

Figure 11: Monthly streamflow validation (2007–2015).

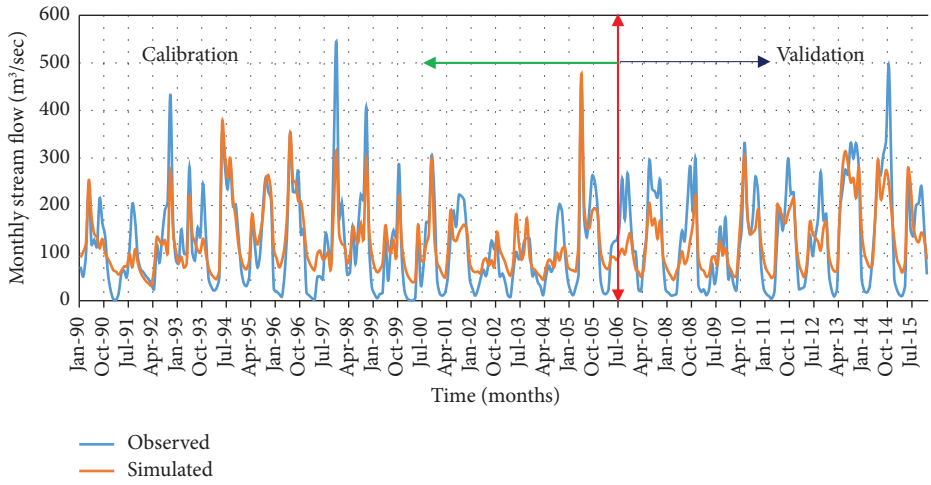

Figure 12: Monthly streamflow calibration and validation (1990–2015).

land-use activities, play a significant role in hydrological modeling. Coarse spatial resolutions may overlook local variations in soil types and land use, vital for predicting how water moves through and interacts with the landscape. This can affect everything from infiltration rates to runoff generation, ultimately impacting the accuracy of the model's output.

In summary, the SWAT model demonstrated successful replication of observed streamflow during both calibration and validation periods, as evidenced by all numerical model performance metrics presented in Table 2. The model's performance meets or exceeds the acceptable calibration standards for hydrology recommended by SWAT developers, specifically $R^2 > 0.6$, NSE > 0.5, and RSR < 0.7 [46]. Additionally, the graphical comparisons between measured and simulated streamflow showed good agreement for both calibration and validation periods, further supporting the model's efficacy.

3.2. Hydrological Water Balance Components of the Genale Dawa-3 Dam Watershed. The hydrological water balance serves as a fundamental governing mechanism for watershed processes, with SWAT functioning as an analytical tool for component assessment. Assessing the water balance is essential in determining a model's suitability for specific applications. SWAT employs the principle of conservation of mass to calculate the annual water budget of the watershed at the selected outlet following streamflow calibration and validation. To evaluate the water balance's contribution to the annual average, the hydrological processes in the study area were quantified for each year. The calibrated model parameters were incorporated into the SWAT model, and a simulation was conducted for the entire base period (1987–2019), including a three-year warm-up period for model initialization.

Analysis of simulated annual water balance components reveals that the Genale Dawa-3 dam watershed receives a mean annual precipitation of 1083.8 mm. The average annual evaporation loss is 700.78 mm, accounting for 64.66% of the total water budget. This high evapotranspiration component aligns with findings from [47] in the Sherigu catchment of Ghana and southern Burkina Faso and is likely due to the high temperatures in the watershed. SUR_Q, GW_Q, and LAT_Q comprise 136.64 mm (12.61%), 102.59 mm (9.47%), and 93.63 mm (8.64%) of the water balance, respectively. The average streamflow (WYLD), a combination of these three components, accounts for 349.9 mm (32.28%) of the annual water budget. Deep percolation (PERCOLATE) and initial SWo contribute 154.11 mm (14.22%) and 93.29 mm (8.61%), respectively. The final SWo was calculated as 10.63 mm, with zero transmission losses (T_loss) for this study. Given the watershed's area (10,264 km^2), the surface water potential is estimated at 1.4 billion cubic meters (BMC), with a groundwater potential of 1.05 BMC, totaling 2.45 BMC in water potential (Figure 13). The validation period showed greater total water yield compared to the calibration period (Table 5), possibly due to increased rainfall during validation.

3.3. Spatial Distribution of Water Balance Components. The spatial distribution of hydrological components reflects the structural organization of flow generation mechanisms within the Genale Dawa-3 dam watershed (Figure 14). Geographic heterogeneity in subwatershed characteristics, including soil type, land use, and DEM, significantly influences watershed water balance dynamics. Due to this spatial variability in watershed parameters, the simulated annual water balance components demonstrate distinct patterns across individual subwatersheds. At the watershed scale, annual precipitation ranges from 579.35 to 1348.01 mm (Figure 14(a)). The northern watershed region receives maximum rainfall, attributed to elevated topography and extensive plantation coverage. Conversely, the southern region near the watershed outlet experiences minimal precipitation, potentially due to lower elevation profiles and reduced vegetation cover (Figure 14(a)).

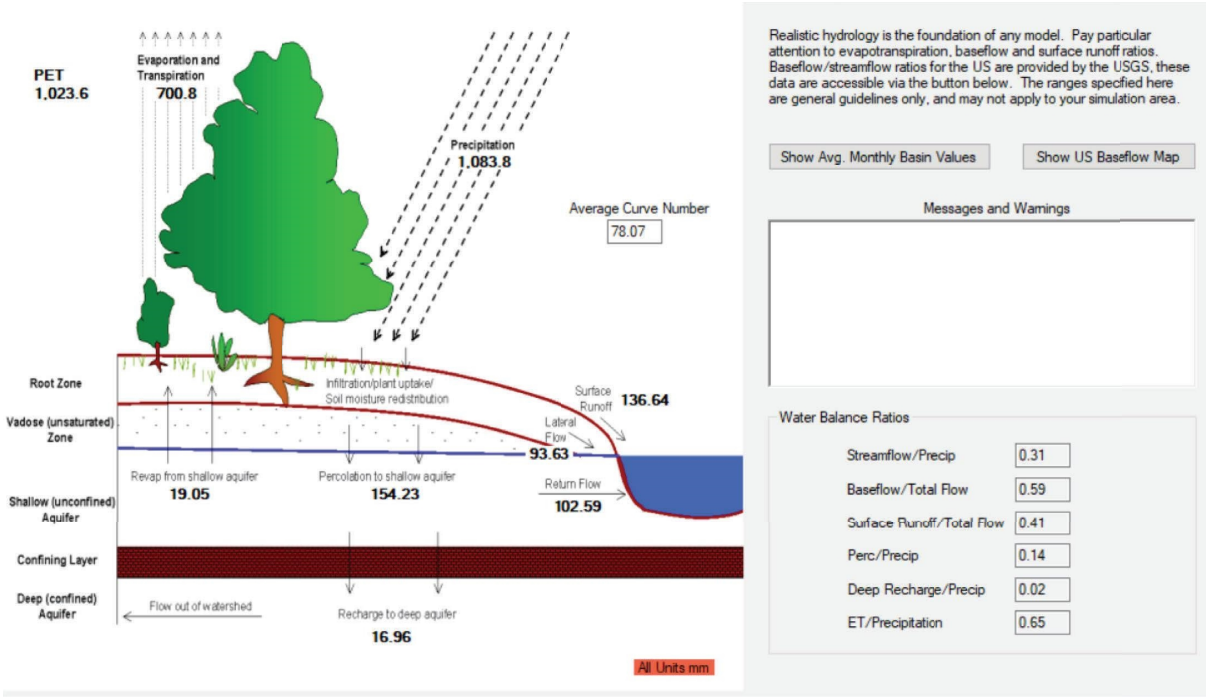

Figure 13: Watershed hydrological components of the Genale Dawa-3 dam.

Table 5: Water balance component simulation during the calibration and validation periods for the Genale Dawa-3 dam watershed (all values are in mm).

Hydrological water balance components	Total time (1990–2015)	Calibration period (1990–2006)	Validation period (2007–2015)
Precipitation	1083.8	1047.69	1131.08
Surface runoff	136.64	134.09	139.95
Groundwater flow	102.62	67.69	148.29
Lateral flow	93.63	90.66	97.51
Evapotranspiration	700.8	699.96	701.79
Water yield	349.90	306.94	406.08

Water yield estimation, a critical parameter for regional water resource management, underwent comprehensive analysis. The subwatershed contribution assessment throughout the simulation period, conducted using the calibrated model framework, revealed results illustrated in Figure 14(b). Water yield variations ranged from 75.18 to 577.98 mm, with maximum values in upstream regions and minimum values near the watershed outlet. The spatial distribution of water production demonstrates a strong correlation with precipitation patterns.

The range of annual evapotranspiration values within the Genale Dawa-3 dam watershed, range from 444.05 to 783.81 mm (Figure 14(c)). The findings of the study indicate that regions characterized by water bodies, shrubs and grasslands, forestland, and low precipitation exhibit the highest average annual evapotranspiration levels. Another contributing factor to the substantial evaporation loss is the rise in temperature, particularly during the dry season. Conversely, areas with settlements and seasonal farming activities experience relatively lower mean annual evapotranspiration rates. Overall, the analysis underscores the significance of evaporation loss as a major component in the water balance of the Genale Dawa-3 dam watershed.

The SWAT model estimated spatial annual SUR_Q values ranging from 40.52 to 369.79 mm across the Genale Dawa-3 dam watershed (Figure 14(d)). The spatial variability in SUR_Q is influenced by several factors, including soil type, vegetation, LULC, slope gradient, groundwater level, rainfall, and other meteorological variables. Based on LULC analysis, this study indicated that the major area of the watershed is dominated by agricultural land, mainly rural villages, which cover 61.11% of the entire area. Soil data analysis, on the other hand, showed that based on texture properties, the distribution of clay textures covers 17.99% of the area: chromic cambisols 2.2%, eutric cambisols 12.35%, and eutric vertisols 3.44%. The other 82.02% consists of loam and sandy loam: chromic luvisols, which make up 50.13%; eutric leptosols, 13.48%; haplic luvisols, 0.34%; humic nitisols, 10.80%; and lithic leptosols, 7.27%. Higher runoff amounts were seen in rural villages and places with clay soil in the study area. Cultivated land was identified as the primary contributor to runoff during the study. This is

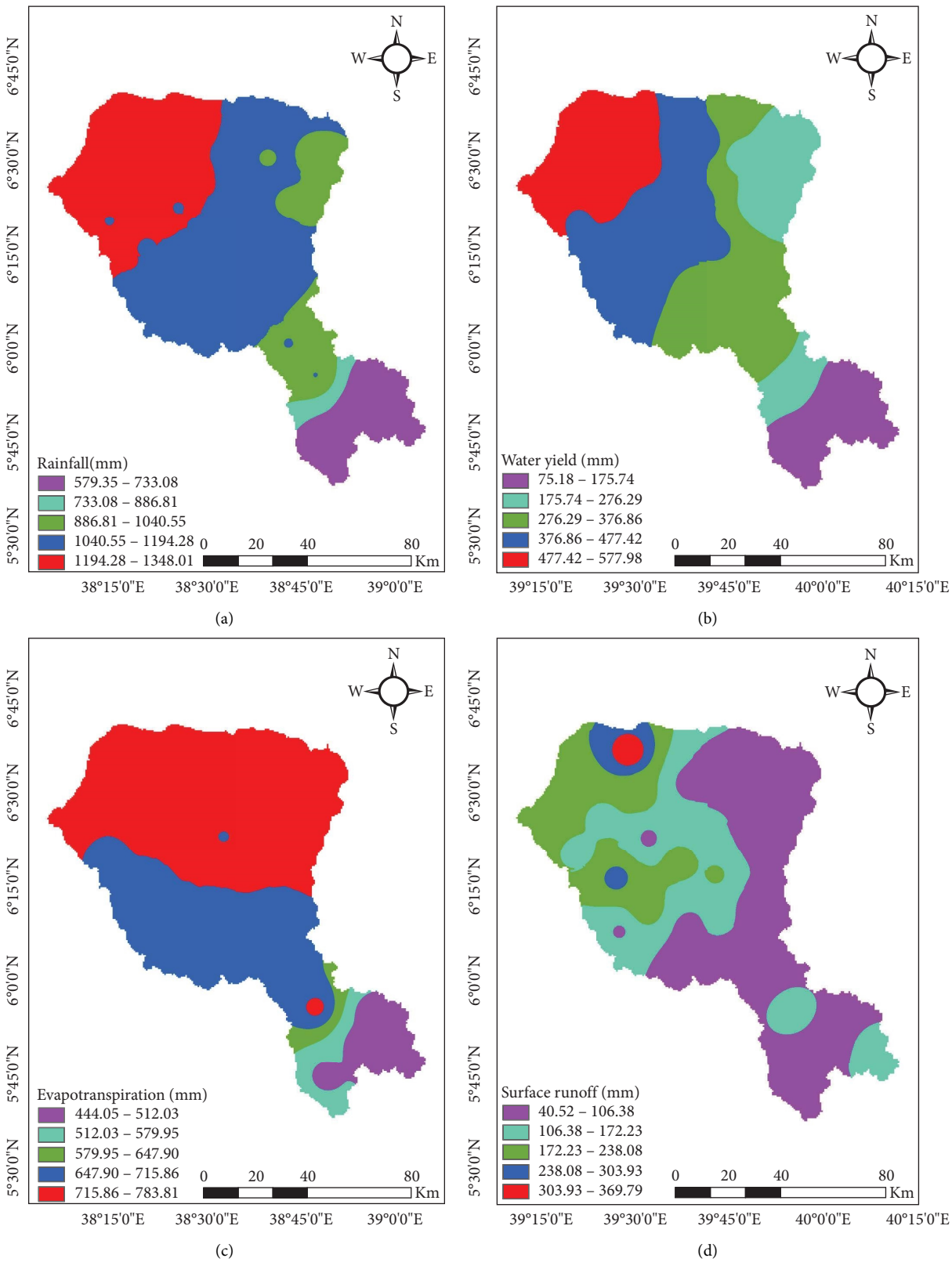

Figure 14: Continued.

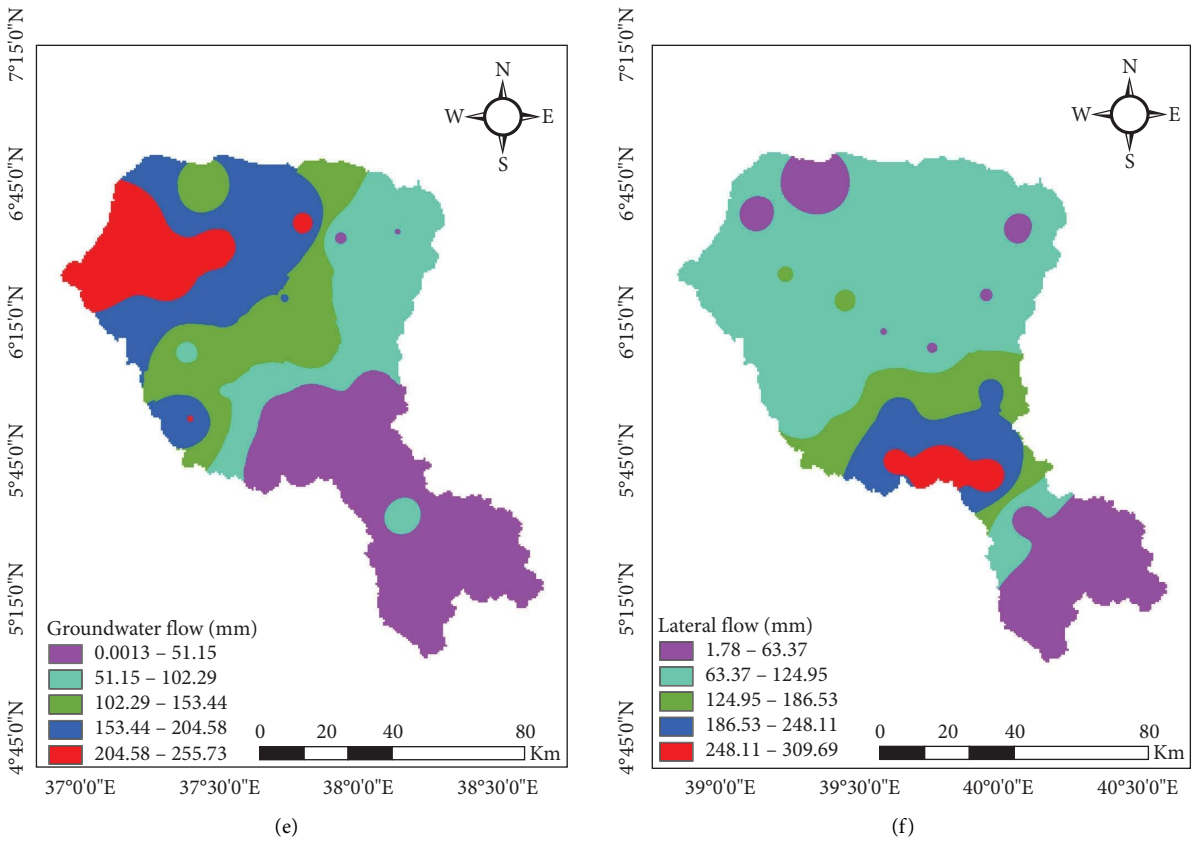

Figure 14: Spatial distribution map of water balance components.

explained by the fact that clay soil has a lower infiltration capacity and that rural settlement areas are more compacted, which lowers the rates of water percolation and recharging. In contrast, areas primarily composed of sandy loam and loam soil with denser vegetation, such as shrubs and forests, demonstrated lower SUR_Q. The prevalence of sandy loam and loam soil in these areas allows for better permeability, enabling soil and water to evaporate or infiltrate rather than being lost through runoff.

The annual groundwater recharge in the Genale Dawa-3 dam watershed of southeastern Ethiopia, as determined by the SWAT model, ranges from 0 to 255.73 mm (Figure 14(e)). According to [48], recharge rates are influenced by multiple factors including vegetation, precipitation characteristics, geological features, topography, and soil properties. Rainfall intensity emerged as the primary driver of spatial heterogeneity in groundwater recharge across subwatersheds. The northern watershed section exhibited maximum recharge variability due to deeper aquifers, permeable soils, and extensive vegetation. Conversely, southern regions near the reservoir inlet showed reduced recharge rates due to alluvial deposits and weathered geology. As a result, runoff is comparatively higher and recharging is lower. In certain places near the reservoir inlet, the groundwater is so near the surface that the recharge value is zero, meaning that the area is already saturated with water up to the surface and is unable to absorb more water into the soil (Figure 14(e)).

The annual spatial variability in LAT_Q ranged from 1.78 to 309.69 mm (Figure 14(f)), which was the minimum percentage of water balance components (8.64%). The minimum LAT_Q was located at the northern and southern tips of the watershed. The low infiltration capacity of water due to development and associated impervious surfaces can lead to increased SUR_Q, which may explain the observed phenomenon. On the other hand, the middle part of the watershed exhibited a significant amount of LAT_Q, likely because of the high infiltration capacity of water and pervious surfaces, which reduce SUR_Q.

3.4. Seasonal (Temporal) Variation of Water Balance Components. The major part of the study area is dominated by mixed agriculture, including crop production and livestock rearing. A major share of crops in the area is produced side by side with rearing livestock. The land use statistics show relatively low population density and less fragmentation of agricultural land. The major crops grown in the project area include maize, sorghum, teff, onion, tomato, pepper, sugarcane, and banana, which are grown on main fields and recession farms. All crops, apart from sorghum and teff, are grown under irrigation and recession farming. In both rain-fed and recession farming, the maize crop occupies the largest area of the household land holding [16]. This classification is challenged by the intensive use of water resources, which in large measure occurs in irrigation and

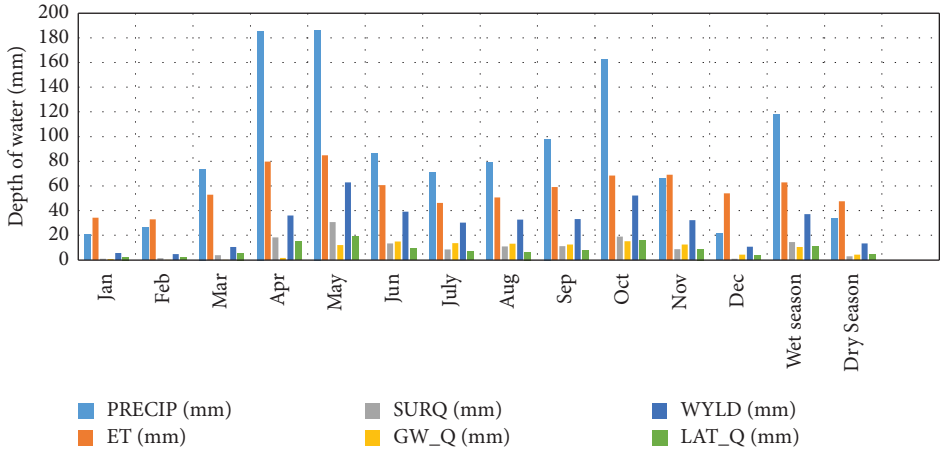

Figure 15: Monthly and seasonal (temporal) variation of water balance components.

farming practices. The key issues include the water demand and supply imbalance, the sustainability of traditional irrigation systems, the impact on water balance, and vulnerability to climate variability. Addressing these challenges requires a detailed understanding of the water balance components in the study area.

Water balance is crucial in the aspects of farming and social practices in wet and dry seasons, respectively; it involves the crucial components of precipitation, evapotranspiration, SUR_Q, groundwater recharge, water yield, and LAT_Q. For this study, the wet season (MAMJJASO) high amount of precipitation allowing rain-fed agriculture with crops that require plenty of water. Farmers also give sufficient attention to surplus water by draining off excess water and storing it in farm ponds for future use. Evapotranspiration rises with the growth of plants, thus supporting the need for practices like nutrient management that optimize water use, while high SUR_Q replenishes rivers, streams, and aquifers through good groundwater recharge. Communities take advantage of this period to harvest water, enhance recharge structures, and mitigate flood risks through embankments and check dams. Conversely, in the dry period (NDJF), which has scattered precipitation, the focus is on conservation and effective utilization of available water. Farmers stored water and groundwater to irrigate, often growing drought-tolerant crops. Various techniques to manage high evapotranspiration and runoff were used, which include mulching and soil bunding. Groundwater has become crucial, and measures for its utilization were used to avoid its depletion. Social perspective, focused on watershed management, rationing water usage, and advocating for sustainable practices to ensure adequate supply. In both seasons, farming and community activities align with the dynamics of water availability, balancing short-term needs with long-term sustainability. The monthly and seasonal (temporal) variations of water balance components of the Genale Dawa-3 dam watershed are illustrated in Figure 15.

4. Conclusions

The SWAT model calibration and validation processes for streamflow simulation in the Genale Dawa-3 dam watershed were accomplished using SWAT-CUP-2019 and SUFI-2 algorithms. During calibration, critical hydrological parameters were identified, encompassing base flow dynamics, initial curve number characteristics, channel conductivity metrics, groundwater delay coefficients, deep aquifer percolation rates, slope length factors, and soil water capacity variables. These parameters were instrumental in optimizing the alignment between simulated outputs and observed measurements. The model performance assessment employed rigorous statistical metrics, including R^2, NSE, RSR, and PBIAS. The quantitative results demonstrated performance ranges of 0.79–0.75 (R^2), 0.74–0.72 (NSE), 0.57–0.56 (RSR), and −2.8% to +2.1% (PBIAS) during calibration and validation phases. The results from both calibration and validation phases indicated high accuracy in streamflow prediction, with the statistical values demonstrating the model's robust performance.

Following calibration, the model was employed to examine the hydrological water balance components of the watershed. This analysis revealed a substantial total water potential of 2.45 BMC, distributed between 1.4 BMC of surface water and 1.05 BMC of groundwater. This thorough evaluation of the watershed's hydrology provides valuable insights that could significantly impact water resource management strategies in the area. The accurate streamflow simulations and detailed water balance analysis provide a solid foundation for developing effective water management strategies. This information can guide decision-making processes related to water allocation, flood control, drought mitigation, and sustainable water use practices.

Furthermore, the insights gained from this study can directly benefit the local community by addressing water-related challenges. The quantification of surface and groundwater potentials can inform infrastructure planning, such as reservoir management and groundwater extraction policies. It can also support agricultural planning, urban water supply strategies, and ecosystem conservation efforts. By providing a clear picture of the watershed's hydrological dynamics, this study empowers stakeholders to make informed decisions that balance human needs with environmental sustainability, potentially improving water security

and resource management in the Genale Dawa-3 dam watershed region.

Data Availability Statement

The data used during the current study are available from the corresponding author upon reasonable request.

Conflicts of Interest

The authors declare no conflicts of interest.

Author Contributions

Ashenafi Dechasa developed the study concept, methodology, and formal analysis. Wakjira T. Dibaba conducted the investigation and provided resources, data curation, and supervision. Alemu O. Aga, Mezgebu Geme Worku, Miliyon Dida Feye, Firaol Bedada Kopesa, and Bekele Terefe Gebisa performed fieldwork, software validation, and supervision. Brook Legese and Amare Tura Abate have paraphrased the entire document and improved its grammar usage. All the authors were involved in writing the reviews and editing the manuscript. All the authors have read and agreed to the published version of the manuscript.

Funding

This research received no external funding.

Acknowledgments

The authors thank Bule Hora and Jimma University for hosting and supporting the study. We also would like to offer special thanks to the Ethiopian Ministry of Water and Energy and the National Meteorological Service Agency (NMSA) of Ethiopia for providing the streamflow and climate data of the study watershed. We sincerely appreciate the local communities and administrative officer's cooperation and support in sharing information during data collection.

References

[1] A. Adamu, "Assessing the Impacts of Land Use and Land Cover Change on Hydrology of Watershed: A Case Study on Gilgel–Abbay Watershed, Lake Tana Basin, Ethiopia" (2013).

[2] S. Demeku, T. Assefa, B. Berhanu, and G. Zeleke, "Impacts of Micro-Basin Water Harvesting Structures in Improving Vegetative Cover in Degraded Hillslope Areas of North-East Ethiopia," *The Rangeland Journal* 31, no. 2 (2009): 259–265.

[3] T. F. Negewo and A. K. Sarma, "Estimation of Water Yield under Baseline and Future Climate Change Scenarios in Genale Watershed, Genale Dawa River Basin, Ethiopia, Using SWAT Model," *Journal of Hydrologic Engineering* 26, no. 3 (2021): 1–13, https://doi.org/10.1061/(ASCE)HE.1943-5584.0002047.

[4] S. Tekleab, S. Uhlenbrook, Y. Mohamed, H. H. G. Savenije, M. Temesgen, and J. Wenninger, "Water Balance Modeling of Upper Blue Nile Catchments Using a Top-Down Approach," *Hydrology and Earth System Sciences* 15, no. 7 (2011): 2179–2193, https://doi.org/10.5194/hess-15-2179-2011.

[5] S. Takele, S. Gebre, G. Gebremariam, and N. Engida, "Hydrological Modeling in the Upper Blue Nile Basin Using Soil and Water Analysis Tool (SWAT)," *Modeling Earth Systems and Environment* 8, no. 1 (2022): 277–292, https://doi.org/10.1007/s40808-021-01085-9.

[6] F. Arai, S. Pereira, and G. Geula, "Characterization of Water Availability in a Hydrographic Basin," *Technical Paper* (2012): 591–601.

[7] K. S. Rautela, M. Kumar, M. S. Sofi, J. C. Kuniyal, and S. U. Bhat, "Modelling of Streamflow and Water Balance in the Kuttiyadi River Basin Using SWAT and Remote Sensing/GIS Tools," *International Journal of Environmental Research* 16, no. 4 (2022): 1–14, https://doi.org/10.1007/s41742-022-00416-7.

[8] M. K. Leta, T. A. Demissie, and M. Waseem, "Analysis of Hydrological Characteristics of Blue Nile Basin, Nashe Watershed," *Applied Sciences* 11, no. 24 (2021): https://doi.org/10.3390/app112411791.

[9] K. L. Larson, C. Polsky, P. Gober, H. Chang, and V. Shandas, "Vulnerability of Water Systems to the Effects of Climate Change and Urbanization: A Comparison of Phoenix, Arizona and Portland, Oregon (USA)," *Environmental Manager* 52, no. 1 (2013): 179–195, https://doi.org/10.1007/s00267-013-0072-2.

[10] S. M. Ghoraba, "Hydrological Modeling of the Simly Dam Watershed (Pakistan) Using GIS and SWAT Model," *Alexandria Engineering Journal* 54, no. 3 (2015): 583–594, https://doi.org/10.1016/j.aej.2015.05.018.

[11] S. A. Alawi and S. Özkul, "Evaluation of Land Use/land Cover Datasets in Hydrological Modeling Using the SWAT Model," *H2O Journal* 6, no. 1 (2023): 63–74, https://doi.org/10.2166/h2oj.2023.062.

[12] T. D. Tasgara and B. Kumar, "Assessment of Land Use/land Cover Change Impact on Streamflow: A Case Study Over Upper Guder Catchment, Ethiopia," *Sustainable Water Resources Management* 9, no. 1 (2022): 0–12, https://doi.org/10.1007/s40899-022-00783-1.

[13] B. C. Tumsa, G. Kenea, and B. Tola, "The Application of SWAT+ Model to Quantify the Impacts of Sensitive LULC Changes on Water Balance in Guder Catchment, Oromia, Ethiopia," *Heliyon* 8, no. 12 (2022): e12569, https://doi.org/10.1016/j.heliyon.2022.e12569.

[14] W. T. Dibaba, T. A. Demissie, and K. Miegel, "Drivers and Implications of Land Use/Land Cover Dynamics in Finchaa Catchment, Northwestern Ethiopia," *Land* 9, no. 4 (2020): 1–20, https://doi.org/10.3390/land9040113.

[15] H. A. Ayele, A. O. Aga, L. Belayneh, and T. W. Wanjala, "Hydrological Responses to Land Use/Land Cover Changes in Koga Watershed, Upper Blue Nile, Ethiopia," *Geographies* 3, no. 1 (2023): 60–81, https://doi.org/10.3390/geographies3010004.

[16] MoWR, "The Federal Democratic Republic of Ethiopia" (Ministry of Water Resources, 2007).

[17] T. Awulachew, A. D. Yilma, M. Loulseged, W. Loiskandl, and M. Ayana, in *Water Resources and Irrigation Development in Ethiopia*, 78 (International Water Management Institute, 2007).

[18] A. Dechasa, A. Aga, and T. Dufera, "Erosion Risk Assessment for Prioritization of Conservation Measures in the Watershed of Genale Dawa-3 Hydropower," *Quaternary* 5, no. 4 (2022): https://doi.org/10.3390/quat5040039.

[19] NASA, *ASTER Global Digital Elevation Map-2018* (2018).

[20] M. A. Degefu, Y. Tadesse, and W. Bewket, "Observed Changes in Rainfall Amount and Extreme Events in Southeastern Ethiopia, 1955–2015," *Theoretical and Applied Climatology*

144, no. 3–4 (2021): 967–983, https://doi.org/10.1007/s00704-021-03573-5.

[21] J. R. W. Neitsch, J. G. Arnold, and J. R. Kiniry, *Soil and Water Assessment Tool* (Theoretical Documentation Version 2005.Temple, Tx.USDA, 2005).

[22] USGS, "Earth Explorer Map-2018," https://earthexplorer.usgs.gov/.

[23] M. Shigute, T. Alamirew, A. Abebe, C. E. Ndehedehe, and H. T. Kassahun, "Understanding Hydrological Processes under Land Use Land Cover Change in the Upper Genale River Basin, Ethiopia," *Water (Switzerland)* 14, no. 23 (2022): https://doi.org/10.3390/w14233881.

[24] OWWDSE, "Oromia Water Works Design, and Supervision Enterprise," https://milkta.com/en/organizations/2161/oromia-water-works-design-and-supervision-enterprise-owwdse.

[25] NMA, "Ethiopia National Meteorological Agency," (2021), http://www.ethiomet.gov.et/stations/information.

[26] A. Angstrom, "Solar and Terrestrial radiation.Report to the International Commission for Solar Research on Actinometric Investigations of Solar and Atmospheric Radiation," *Quarterly Journal of the Royal Meteorological Society* 50, no. 210 (1924): 121–126, https://doi.org/10.1002/qj.4970502/008.

[27] MoWE, "Ministry of Water and Energy," (2021), https://mowe.gov.et/.

[28] S. L. N. Arnold, J. G. J. R. Kiniry, R. Srinivasan, J. R. Williams, and E. B. Haney, *Soil Water Assessment Tool (SWAT)theoretical Documentation Version 2012*, Technical Report No.439 (College Station, TX: Texas Water Resources Institute, 2012).

[29] J. R. Neitch, J. R. Arnold, J. R. Kiniry, and Williams, *Soil and Water Assessment Tool (SWAT) Theoretical Documentation Version2009. Texas Water Resources Institute*, Technical Report No.406 (College Station, Texas: Texas A&M University System, 2011).

[30] USDA, "National Engineering Handbook," *Hydrology Section*, 4 (1972).

[31] M. Dananto, A. O. Aga, and P. Yohannes, "Assessing the Water-Resources Potential and Soil Erosion Hotspot Areas for Sustainable Land Management in the Gidabo Watershed, Rift Valley Lake. Basin of Ethiopia," *Sustainability* (2022): https://doi.org/10.3390/su14095262.

[32] K. White and I. Chaubey, "Sensitivity Analysis, Calibration, and Validations for a Multisite and Multivariable SWAT Model," *Journal of the American Water Resources Association* 41, no. 5 (2005): 1077–1089, https://doi.org/10.1111/j.1752-1688.2005.tb03786.x.

[33] A. van Griensven, T. Meixner, S. Grunwald, T. Bishop, M. Diluzio, and R. Srinivasan, "A Global Sensitivity Analysis Tool for the Parameters of Multi-Variable Catchment Models," *Journal of Hydrology* 324, no. 1–4 (2006): 10–23, https://doi.org/10.1016/j.jhydrol.2005.09.008.

[34] K. Abbaspour, "User Manual for SWAT-CUP, SWAT Calibration and Uncertainty Analysis Programs," *Swiss Federal Institute of Aquatic Science and Technology* (Switzerland: Duebendorf, 2014).

[35] S. Swain, "Hydrological Modeling Through SWAT over a Himalayan Catchment Using High-Resolution Geospatial Inputs," *Environmental Challenges* 8 (2022): 100579, https://doi.org/10.1016/j.envc.2022.100579.

[36] D. N. Moriasi, M. W. Gitau, N. Pai, and P. Daggupati, "Hydrologic and Water Quality Models: Performance Measures and Evaluation Criteria," *Journal of Agricultural and Biological Engineering* 58, no. 6 (2015): 1763–1785, https://doi.org/10.13031/trans.58.10715.

[37] P. Krause, D. P. Boyle, and F. Bäse, "Comparison of Different Efficiency Criteria for Hydrological Model Assessment," *Advances in Geosciences* 5 (2005): 89–97, https://doi.org/10.5194/adgeo-5-89-2005.

[38] J. E. Nash and J. Sutcliffe, "River Flow Forecasting Through Conceptual Models, Part I. A Discussion of Principles," *Journal of Hydrology* 10, no. 3 (1970): 282–290.

[39] W. T. Gupta, "Model Calibration and Uncertainty Estimation," *Encyclopedia of Hydrological Sciences* 11, no. 131 (2005): 1–17.

[40] H. Lemma, E. Adgo, J. Poesen, and J. Nyssen, "Identifying Erosion Hotspots in Lake Tana Basin From a Multisite Soil and Water Assessment Tool Validation: Opportunity for Land Managers" (2019), 1449–1467, https://doi.org/10.1002/ldr.3332.

[41] T. Gashaw, "Evaluating the Effectiveness of Best Management Practices on Soil Erosion Reduction Using the SWAT Model: for the Case of Gumara Watershed, Abbay (Upper Blue Nile) Basin," *Environmental Management* 2006 (2021): https://doi.org/10.1007/s00267-021-01492-9.

[42] W. T. Dibaba, T. A. Demissie, and K. Miegel, "Prioritization of Sub-watersheds to Sediment Yield and Evaluation of Best Management Practices in Highland Ethiopia, Finchaa Catchment," *Land* 10, no. 6 (2021): https://doi.org/10.3390/land10060650.

[43] T. Kefay, T. Abdisa, and B. Chelkeba, "Prioritization of Susceptible Watershed to Sediment Yield and Evaluation of Best Management Practice: A Case Study of Awata River, Southern Ethiopia," *Applied and Environmental Soil Science* 2022 (2022): https://doi.org/10.1155/2022/1460945.

[44] W. T. Dibaba and D. G. Ebsa, "Identifying Erosion Hot Spot Areas and Evaluation of Best Management Practices in the Toba Watershed, Ethiopia," *Water Conservation & Management* 6, no. 1 (2022): 30–38, https://doi.org/10.26480/wcm.01.2022.30.38.

[45] A. Fadil, H. Rhinane, A. Kaoukaya, Y. Kharchaf, and O. Bachir, "Hydrologic Modeling of the Bouregreg Watershed (Morocco) Using GIS and SWAT Model," *Journal of Geographic Information System* 03, no. 04 (2011): 279–289, https://doi.org/10.4236/jgis.2011.34024.

[46] C. Santhi, J. G. Arnold, J. R. Williams, W. A. Dugas, R. Srinivasan, and L. M. Hauck, "Validation of the SWAT Model on a Larger River Basin With Point and Nonpoint Sources," *Journal of the American Water Resources Association* 37, no. 5 (2001): 1169–1188.

[47] S. Guug, S. Ganiyu, and A. Kasei, "Application of SWAT Hydrological Model for Assessing Water Availability at the Sherigu Catchment of Ghana and Southern Burkina Faso," *HydroResearch* 3 (2020): 124–133, https://doi.org/10.1016/j.hydres.2020.10.002.

[48] G. B. Tesfahunegn and P. L. G. Vlek, "Application of SWAT Model to Assess Erosion Hotspot for Sub-Catchment Management at Mai-Negus Catchment in Northern Ethiopia" (2013).